RSC Advances

ROYAL SOCIETY OF CHEMISTRY

www.rsc.org/advances

Journal Name

ARTICLE

Spirochromone-chalcone conjugates as antitubercular agents: synthesis, bio evaluation and molecular modeling studies

Received 00th January 20xx,
Accepted 00th January 20xx

DOI: 10.1039/x0xx00000x

www.rsc.org/

M. Mujahid,[a] P. Yogeeswari,[b] D. Sriram,[b] U. M. V. Basavanag,[c] Erik Díaz-Cervantes,[c] Luis Córdoba-Bahena,[c] Juvencio Robles,[c] R. G. Gonnade,[a] M. Karthikeyan,[a] Renu Vyas,[a] M. Muthukrishnan*[a]

A new series of spirochromone annulated chalcone conjugates were synthesized and evaluated for their antitubercular activity against Mycobacterium tuberculosis H37Rv strain. These compounds were subjected to molecular modeling studies using docking and chemoinformatics based approaches. The docking simulations were performed against a range of known receptors for chalcone derived compounds to reveal MTB phosphotyrosine phosphatase B [MtbPtpB] protein as the most probable target based on the high binding affinity scores. Five compounds exhibit significant inhibition, showing minimum inhibitory concentration values i.e. MIC values ranging from 3.13-12.5 µg/ml. Further analysis of the synthesized compounds with known and in-house developed chemoinformatics tools unequivocally established their potential as anti-tubercular compounds. QSAR modeling revealed a quantitative relationship between biological activities and frontier molecular orbital energies of synthesized compounds. The predictive model can be employed further for virtual screening of new compounds in this series.

Introduction

Tuberculosis is a devastating bacterial disease caused by *Mycobacterium tuberculosis* (Mtb). It poses a major public health risk due to the long duration of treatment (6-9 months), coinfection with HIV and the emergence of multidrug resistant strains etc. According to a WHO report, in 2013 alone, nearly 9 million people contracted tuberculosis and 1.5 million died from complications of the disease.[1] Despite enormous efforts to develop antimycobacterial drug molecules, tuberculosis still constitutes the leading killer disease. Therefore, the discovery and development of new types of anti TB agents acting on novel drug targets is urgently needed.

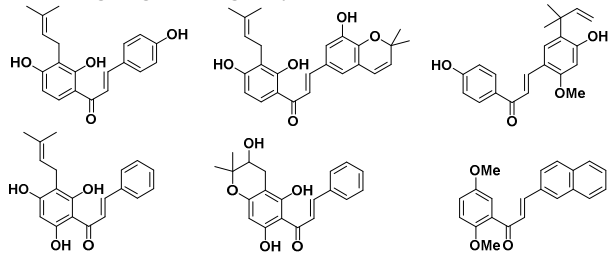

Figure 1.Natural/NP inspired chalcones with potent activity against *Mtb*

It is a well known fact that biologically active natural products are recognized as evolutionarily selected and biologically prevalidated starting point for any successful drug discovery program. Therefore, the synthesis of natural products inspired compound collections and their biological evaluation is a highly promising strategy for the identification of unique biologically relevant compound classes, especially in the studies aimed at finding a new class of anti TB agents.[2] Flavonoids are the most explored class of natural products as they are widely distributed in various plants and foods such as fruits & vegetables.[3] Chalcones are an important sub class of flavonoids that consist of open chain flavonoids in which the two aromatic rings are fused by a three-carbon α,β-unsaturated carbonyl system.[4] They have been reported to possess plethora of medicinal applications which include anti-inflammatory, antileukemic, antiulcerogenic, antimalarial, antileishmaniosis, and anticancer activities.[5] Interestingly, many natural and natural product inspired chalcone analogues exhibit significant antimycobacterial activity (Figure 1).[6] Recently, several research groups successfully demonstrated their mode of action by identifying their molecular targets.[7]

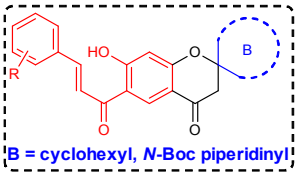

Figure 2. Design of spirochromone annulated chalcone conjugates

[a] CSIR-National Chemical Laboratory, Dr. Homi Bhabha Road, Pune, Maharashtra, India- 411008. E-mail: m.muthukrishnan@ncl.res.in; Fax: +91-20-25902629; Ph:+91-20-25902284
[b] Medicinal Chemistry & Antimycobacterial Research Laboratory, Pharmacy Group, Birla Institute of Technology & Science – Pilani, Hyderabad Campus, Jawahar Nagar, Hyderabad 500 078, India
[c] Departamento de Química y Departamento de Farmacia, Universidad de Guanajuato, Noria Alta S/N, Col. Noria Alta, C.P. 36050, Guanajuato, Gto., México

†Electronic Supplementary Information (ESI) available: CCDC 1045946 (**4f**). Characterization of new compounds and crystallographic data or other electronic format See DOI: 10.1039/b000000x

A good safety profile, possibility of oral administration,[8] and easy synthesis are the major factors contributing to the growing interest in exploring the pharmacological activities of chalcones. In this context, and in view of our long standing interest in the chemistry of the privileged chromone motif,[9] we recently reported various spirochromone derivatives possessing 1,2,3-triazole and amino alcohol moieties that can serve as lead molecules for developing antitubercular agents.[10] These results encouraged us to further explore the spirochromone motif as an active pharmacophore for further diversification to exploit its anti TB potential. Herein, we describe the synthesis of novel spirochromone annulated chalcones, their in silico studies and *in vitro* screening results against *Mycobacterium tuberculosis* H37Rv (Figure 2). To the best of our knowledge, no reports on the synthesis, in silico study and antimycobacterial activities of these spirochromone annulated chalcone have been reported.

Results and discussion

Synthesis

A three step synthetic strategy was followed for the preparation of spirochromone annulated chalcones as outlined in **Scheme 1**. As shown, the readily available resorcinol **1** on heating with acetic anhydride in the presence of anhydrous zinc chloride provided 4,6-diacetyl resorcinol **2** in 75% yield.[11] The diacetyl compound **2** on Kabbe condensation with cyclohexanone or *N*-Boc piperidone in the presence of pyrrolidine as a base in refluxing toluene using Dean-Stark apparatus provided spirochromone derivatives **3a** and **3b** in 62% and 65% yields. Lastly, spirochromone derivatives **3a,b** on treatment with various aryl aldehydes using Claisen–Schmidt condensation reaction produced spirochromone annulated chalcones **4a-g** & **5a-h** in moderate to good yields. The structure of all the new products **4** & **5** (15 compounds) was confirmed by ^{1}H NMR, ^{13}C NMR and mass spectral analysis. For an example, in the ^{1}H NMR spectra (compound **4f** as a representative example), a signal corresponding to the C-3 protons of chromanone skeleton was observed as a singlet at δ 2.73 ppm and the corresponding ^{13}C resonance signal was observed at δ 47.8 ppm and the spirocarbon was discernible at δ 81.4 ppm. Further, the appearance of a sharp singlet (1H) observed at δ 13.5 ppm in the PMR, suggested the presence of one chelated hydroxyl group. In addition, the appearance of two sets of doublets at δ 7.61 & 7.87, 1H each with coupling constant 15.4 Hz were ascribable to the olefinic protons of the chalcone moiety. Conclusive evidence for its structure was derived from a single crystal X-ray analysis (**Figure 3**).

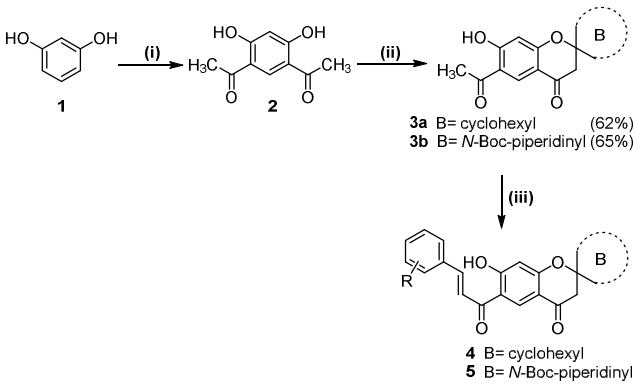

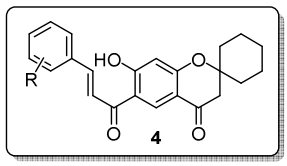

	R	
4a	4-F	(68%)
4b	2-F	(72%)
4c	2-Cl	(65%)
4d	4-OMe	(65%)
4e	2, 4-dimethoxy	(78%)
4f	3-methoxy	(75%)
4g	3-piperonal	(76%)

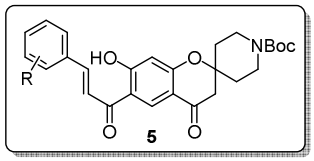

	R	
5a	C_6H_5	(80%)
5b	4-F	(68%)
5c	2-F	(74%)
5d	2-Cl	(70%)
5e	3-OMe	(64%)
5f	4-OMe	(65%)
5g	2, 4-dimethoxy	(71%)
5h	2,5-dimethoxy	(72%)

Scheme 1. Reagents and conditions: (i) Ac_2O, $ZnCl_2$, 140°C,30 min, 75%; (ii) Cyclohexanone/N-Boc-piperidone, pyrrolidine, toluene, reflux, 12 h; (iii) aromatic aldehyde, 50 % aq. KOH, MeOH

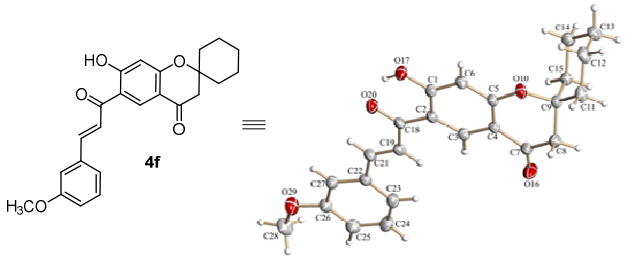

Figure 3. ORTEP diagram of the compound **4f**

Anti-mycobacterial evaluation

All the new spirochromone annulated chalcone conjugates were screened for their *in vitro* antimycobacterial activity against *M. tuberculosis* H37Rv (ATCC27294) using an agar dilution method. The minimum inhibitory concentration (MIC; µg/mL) was determined for each compound. The MIC is defined as the minimum concentration of compound required to completely inhibit the bacterial growth. Rifampicin and ethambutol were used as reference compounds. The MIC values of the synthesized compounds along with the standard drugs for comparison are reported in **Table 1**.

Among the 15 spirochromone annulated chalcone conjugates tested, five compounds **4a, 4b, 5b, 5c**, and **5d** were shown to be active with MIC values in the range of 3.13-12.5 µg/mL. The compound **5c** is shown to be highly active among all the compounds tested with a MIC value of 3.13 µg/mL. It has a core spirochromone moiety hitherto unreported.The preliminary SAR of the spirochromone annulated conjugates

reveals that compounds possessing piperidinyl group at 2nd position of the chromone ring favors better activity than the cycloalkyl group. In addition, the activity is being influenced by functional groups present in the chalcone moiety as well. Halogen substitution at aromatic ring, especially fluoro substitution enhances the activity (**5b**, **5c**). It is also observed that the presence of methoxy substitution at aromatic ring doesn't seem to influence the activity.

Table 1: *In vitro* antimycobacterial activity of the spirochromone annulated chalcone conjugates

Entry	Compound	MIC (μg/mL)	Entry	Compound	MIC (μg/mL)
1	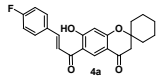	12.5	10	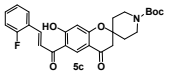	3.13
2	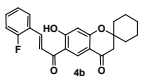	12.5	11	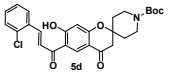	12.5
3	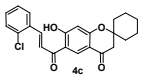	25	12	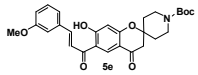	25
4	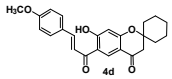	>25	13	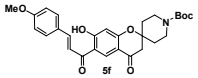	25
5	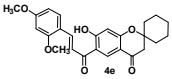	>25	14	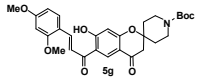	25
6	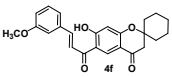	>25	15	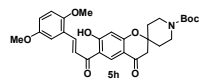	>25
7	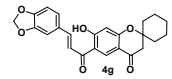	>25	16	Rifampicin	0.2
8	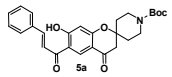	>25	17	Ethambutol	1.56
9	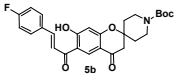	6.25			

Computational studies

Methodology

Preparation of ligands

The 2D structures of all compounds *i.e*. native ligand, compounds **4a**, **4b**, **5b-d**, rifampicin and ethambutol were drawn and analyzed by Marvin view. The compounds were converted to 3D structure (.pdb) using Marvin suite 15.[12] The 3D coordinates (.pdb) of each molecule were loaded on AutoDock tools 1.5.6 (ADT) for energy minimization. Gasteiger charges were added and the rotatable bonds were set by the ADT and all torsions were allowed to rotate.

Preparation of macromolecule

The protein targets retrieved from RCSB Protein Data Bank are proteins associated with metabolic functioning and proliferation of *Mycobacterium tuberculosis*. Enzymes MTB phosphotyrosinephosp hatase A [MtbPtpA] (PDB code 1U2P) and MTB phosphotyrosine phosphatase B [MtbPtpB] (PDB code 2OZ5) proteins, Enoyl acyl carrier protein (PDB code 2NSD), Dihydrofolate reductase (PDB code 1DG5) served as the docking receptors. All the bound ligands and water molecules were removed from the receptors. Polar hydrogen atoms were added and Kollman charges were assigned to the proteins using AutoDock tools (ADT).

Table2: Molecular docking analysis of four protein targets with selected compounds. The binding energies were calculated using MOE and Autodock Vina algorithms. The energy is measured in kcal/mole

	Compound **4a**		Compound **4b**		Compound **5b**		Compound **5c**		Compound **5d**	
PDB target	MOE	Autodock Vina	MOE	Autodock Vina	MOE	Autodock Vina	MOE	Autodock Vina	MOE	Autodock Vina
1U2P	-10.00	-7.10	-9.65	-6.80	-9.98	-6.90	-10.15	-7.60	-11.25	-8.00
2OZ5	-12.41	-8.16	-12.37	-8.30	-13.90	-8.90	-13.96	-9.00	-11.36	-8.30
2NSD	-12.20	-8.10	-11.84	-7.80	-12.95	-8.30	-12.37	-7.10	-12.51	-6.80
1DG5	-12.79	-8.40	-12.47	-8.28	-12.41	-8.00	-11.80	-8.00	-10.40	-7.90

Journal Name

ARTICLE

Table 3: Molecular docking studies of selected compounds on 2OZ5

Entry	Compound ID	Intermolecular distance (Å)	Amino acids involved in intermolecular interactions	Ligand Atom	Receptor Atom	Binding Energy (kcal/mol)
1	Native Ligand	1.40 1.01 3.48 3.07 2.62	Tyr125 Arg59 Arg166 Ser57 Glu129	H2572 O2560 C2512 C2528 O2558	OH1069 NH543 NE1475 OG522 CG1104	-9.2
2	4a	2.96 2.96 2.89 2.44	Ser57 Ser57 His94 Arg166	O2536 O2536 O2534 O2541	OG522 OG522 ND847 NH1481	-8.2
3	4b	2.31 2.76	His94 Tyr125	H2537 O2541	O843 O1069	-8.3
4	5b	3.53	Arg166	O2512	NH1481	-8.9
5	5c	2.52 2.52 2.23	Ser57 Ser57 Glu60	O18 O18 H43	OG585 OE621 OG585	**-9.0**
6	5d	2.78 2.55	Ser57 Lys164	O2543 O2527	OG522 NZ1454	-8.3
7	Rifampicin	1.69 3.53 1.40 2.48 2.76 2.94	Glu60 Phe80 Tyr125 Tyr125 Arg166 Arg166	H2620 H2627 O2519 O2522 O2520 O2521	Oe557 O738 OH1069 OH10c69 NH1478 NH1478	-7
8	Ethambutol	3.07 2.41	Arg166 Phe161	O2512 O2512	N1422 NH1481	-7.8

Molecular docking

The molecular docking was performed and analyzed using two state of art docking algorithms AutoDock Vina[13] and MOE.[14] Lamarckian genetic algorithm method implemented in the program suite was employed to identify appropriate binding modes and conformation of the ligand molecules. The grid map was centered at the active site of the protein by Autogrid. The Lamarckian genetic algorithm, the pseudo-Solis and Wets methods were applied for minimization using default parameters. Binding energy, intermolecular amino acids and their distance were recorded in each ligand bound conformations. In the MOE docking simulations, the ligands were allowed flexibility, London dG scoring function was employed and top 30 conformations were retained.

Molecular docking analysis

With an objective to explore the potential putative targets of the synthesized compounds among the validated Mycobacterium receptors, we performed a docking analysis with known biological targets reported so far for the chalcone scaffold derived anti-tubercular compounds. In general, the validated Mtb targets for this class of compounds are phosphotyrosine phosphatases(MtbPtp A and B; PDB ID: 1U2P, 2OZ5), dihyrdofolate reductase (DHFR), PDB ID: 1DG5) and enol acyl carrier reductases (PDB ID: 2NSD).[15] Accordingly, automated docking was used to assess the binding modes and conformation of the compounds synthesized in this study. Among the 15 spirochromone-chalcone structures, compounds **4a**, **4b**, **5b**, **5c** and **5d** were considered for docking simulations since they exhibited higher anti-tubercular activity, as ascertained from their MIC data (**Table 1**). The four spirochromone chalcones were cross docked against all potential protein targets to reveal better binding affinities with 2OZ5, a MTB phosphotyrosine phosphatase B [MtbPtpB] protein (**Table 3**). PtpB and PtpA are protein tyrosine phosphatases, a class of regulatory enzymes that are secreted by Mtb into the cytosol of infected macrophages. MtbPtpB catalyzes the dephosphorylation of serine/threonine or tyrosine and also has phosphoinositide phosphatase activity whereas PtpA specifically dephosphorylates the tyrosine residues. PtpA inhibits macrophages microbial activity by entering into host macrophages, dephosphorylates the cytoplasmic protein VPS33B and inhibits the phagosome maturation.[16] MtbPtpB blocks the signal regulated kinase and p-38 mediated by IL-6 thereby promoting mycobacterial survival in the host.

PtpA specifically PtpA and PtpB proteins share a structural homology and the active site of the phosphatase enzymes lies in

the P-loop region. However, there are certain differences in the P-loop region and some sequential and positional variations occur in the variable loop. These subtle distinctions in the active sites may account for the high selectivity of the five compounds to MtbPtpB (PDB ID: 2OZ5) than MtbPtpA (PDB ID: 1U2P). Moreover the active site volume computed (CASTp server) showed a greater volume of the binding pocket of PtpB (1509.9 A^3) relative to PtpA (108.7 A^3) enzyme. The present compounds possess volumes ranging from 300-400 A^3 which enables a better fit in the binding pocket of B compared to A. Compound **5c** performed better in the docking run when compared with other synthesized compounds with binding scores ranging from -7.6 to -8.0 kcal/mol against the resolved crystal structure of 2OZ5. In another docking run, the synthesized molecule **5c** chosen for computational studies showed comparable performance with the native ligand of receptor (entry 1**, Table 3**) and slightly better performance than the known MTB drug molecules rifampicin and ethambutol in terms of binding efficiencies (entries 5 and 6**, Table 3**). It is to be noted here that the compound **5c** also possesses the best inhibitory activity in the Mtb assay. Further, the top docked conformation of this compound depicted a greater alignment with the native ligand pose (**Figure 6B**). Hence it is likely to act as good binder for the phosphatase receptor in mycobacterium.

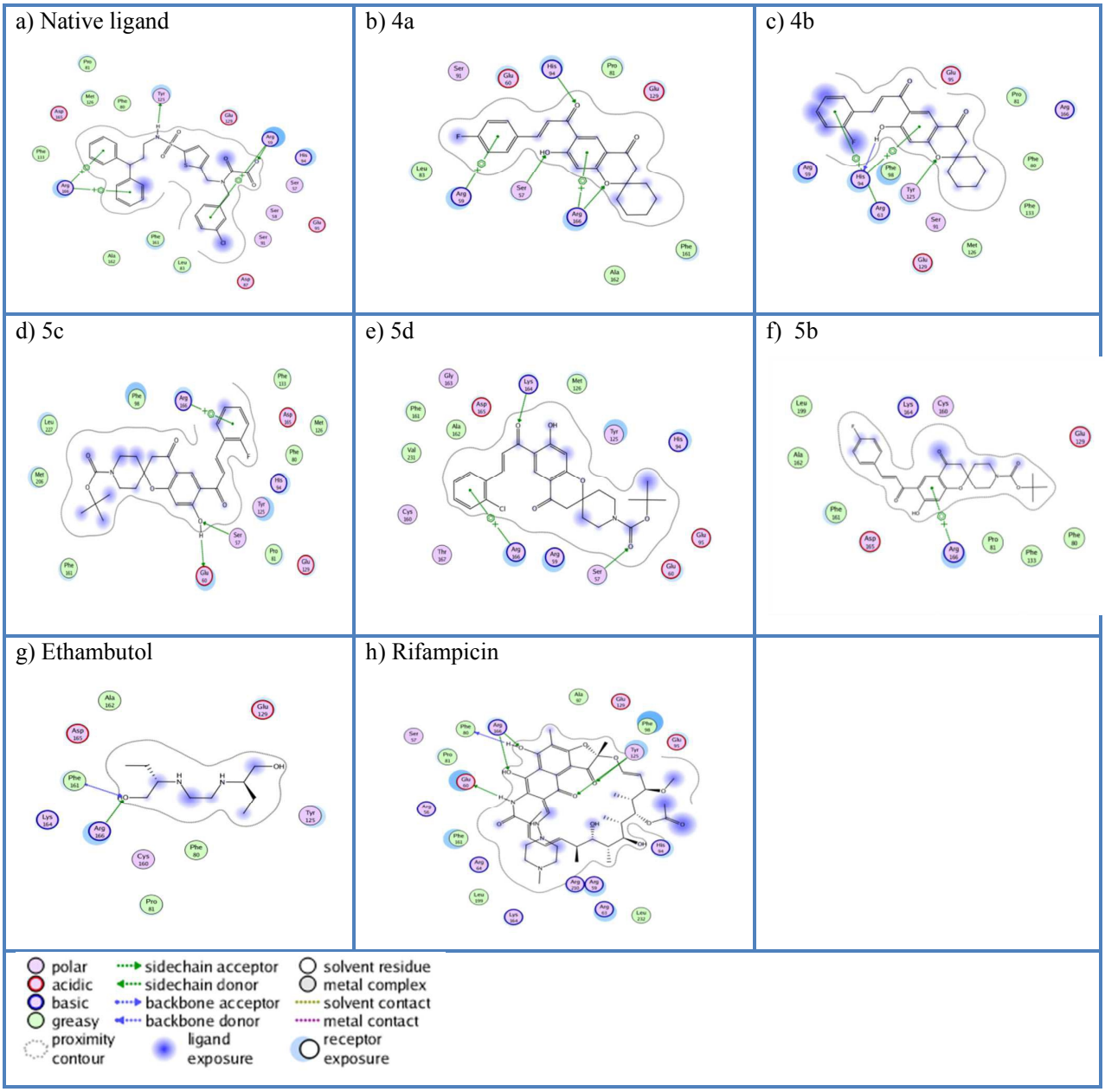

Figure 4: 2D protein ligand interaction maps of compounds **4a, 4b, 5b-5d**, native molecule and known tuberculosis drugs ethambutol and rifampicin.

Journal Name

ARTICLE

The key intermolecular interactions between selected compounds and known drugs against the phosphatase B enzyme are depicted in **Figure 4**. Tyr125, Arg56, Arg166, Ser57 and Glu129 amino acids in the active site interacted with native ligand with many residues depicting a high ligand exposure in the interaction map.[17] Tyr125 acts as hydrogen donor whereas Arg66 acts as hydrogen acceptor and forms a bond with the O group of the ligand. Carbonyl and hydroxyl group based interactions were common in most of the predicted binding poses of compounds in the active site pocket. Specifically, Ser57 of compound **4a**, Glu60 of compound **5c**, Phe80and Arg166 of rifampicin and Arg166 and Phe161 of ethambutol made contacts with the hydroxyl group. Thr125 residue in the receptor pocket interacted with the two carbonyl groups present in the rifampicin structure (entry f**, Figure 4**). Apart from hydrogen bonding, other stablizing intermolecular interactions such as π-cation interaction were also observed.

Figure a:

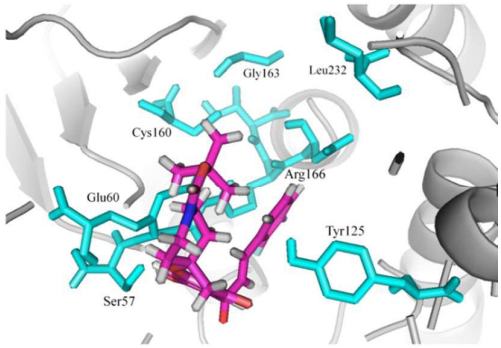

Figure b:

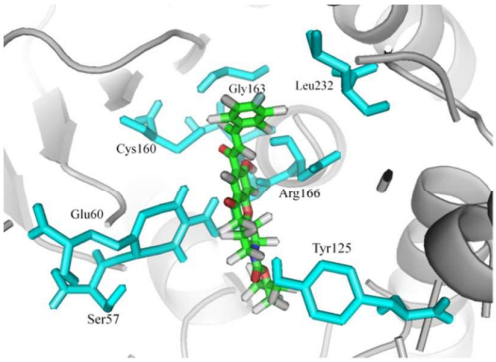

Figure 5: Stereoview depicting the binding mode of compounds 5b and 5c that showed high *in vitro* anti-mycobacterial activity. Figure a depicts compound 5c in magenta, the pocket residues are shown in cyan. Figure b depicts compound 5b in green along with the neighbouring residues (cyan).

Arginine residue was mainly involved in π-cation interaction in the pocket region which helped to stabilize the protein ligand complex formation. Arg166 and Tyr125 were found to interact with the oxygen atom of the pyranone ring system in compounds **4a** and **4b**. Compound **5b** showed a slightly

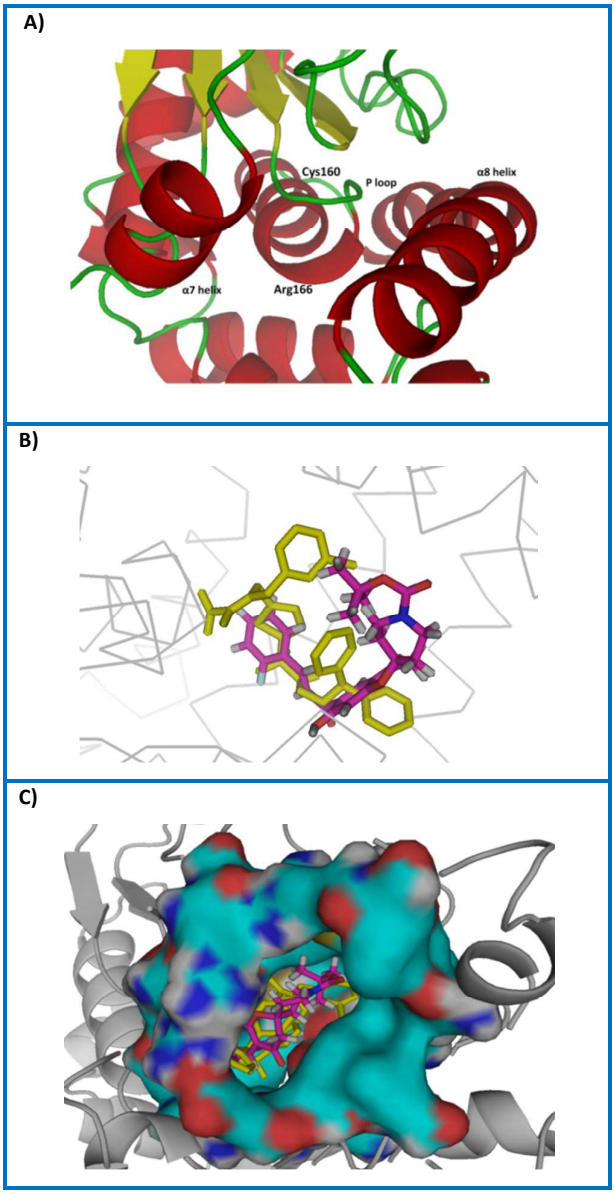

Figure 6: Superposed docking poses for A) Pocket region of 2OZ5 with loops (green) flanked by alpha helices(red) and beta sheets(yellow). B) Structure alignment of docked conformation of Compound 5c (magenta)with native ligand conformation (yellow) in the crystal structure C) Compound 5c and native ligand in the binding pocket of receptor. The receptor surface shown is coloured according to the electrostatic potential.

Table 4: Chemoinformatics analysis of the 15 spirochromone annulated chalcone conjugates

Properties	Compounds														
	4a	**4b**	4c	4d	4e	4f	4g	5a	**5b**	**5c**	**5d**	5e	5f	5g	5h
Lipinski Rule of Five [a]															
Molecular weight	380.41	380.41	396.87	392.45	422.47	392.45	406.43	463.53	481.51	481.52	497.97	493.55	493.55	523.58	523.58
HB accept	4	4	4	5	6	5	6	5	5	5	5	6	6	7	7
HB donor	1	1	1	1	1	1	1	1	1	1	1	1	1	1	1
LogP	5.442	5.442	5.881	5.247	5.238	5.284	4.996	4.911	5.064	5.062	5.501	4.904	4.867	4.858	4.858
Chemical properties															
Weiner path [b]	4228	4228	2152	2464	2912	2422	2664	3910	4284	4228	4228	4637	4693	5384	5332
Ring count [a]	4	4	4	4	4	4	5	4	4	4	4	4	4	4	4
PDL/PLL [a]	0.25	0.25	0.25	0.25	0.25	0.25	0.25	0.25	0.25	0.25	0.25	0.25	0.25	0.25	0.25
ADME properties															
BBB (-3.0 – 1.2) [c]	0.794	0.83	1.62	0.2	0.08	0.22	0.057	0.04	0.07	0.058	0.061	0.03	0.083	0.192	0.074
Caco2 (nms) (<25, poor, >500, best) [c]	31.67	30.74	24.03	37.38	41.81	21.94	24.79	33.27	31.81	31.33	24.31	33.43	36.71	39.38	37.02
HIA (50-100%) [c]	98.01	96.01	96.36	96.25	96.66	96.25	96.73	97.14	97.13	97.13	96.75	97.67	97.67	89.66	98.03
Rotatable bonds (0 - 15)[a]	3	3	3	4	5	4	3	4	4	4	4	5	5	6	6
TPSA (7.0 – 200.0) [b]	93.13	93.14	63.59	72.83	82.05	72.83	82.05	93.13	93.13	93.13	93.13	102.37	102.37	111.6	111.6
Toxicity properties [d]															
DSSTox Carcinogenic potency Mutagenecity	Neg. (C:0.129)	Neg. (C:0.102)	Neg. (C:0.115)	Neg. (C:0.153)	Neg. (C:0.153)	Neg. (C:0.196	Neg. (C:0.129	Neg. (C:0.129	Neg. (C:0.169	Neg. (C:0.153)	Neg. (C:0.129	Neg. (C:0.129	Neg. (C:0.129	Neg. (C:0.169	Neg. (C:0.169
DSSTox Carcinogenic potency Mouse	Neg. (C: 0.080)	Neg. (C: 0.080)	Neg. (C: 0.011)	Neg. (C: 0.011)	Neg. (C: 0.011)	Neg. (C: 0.011)	Neg. (C: 0.085)	Neg. (C: 0.085)	Neg. (C: 0.085)	Neg. (C: 0.011)	Neg. (C: 0.085)	Neg. (C: 0.085)	Neg. (C: 0.085)	Neg. (C: 0.085)	Neg. (C: 0.085)

[a] Computed using Screening Assistant (SA2) program. PDL (Progressive drug like), PLL(Progressive lead like). [b] Calculated using MOE(CCG) Chemoinformatics suite. [c] PreADMET software. [d] LAZAR wherein Neg = Negative and C = Confidence value.

lower docking energy than **5c** (**entry 4, Table 3**). Interestingly, both possess similar structures, the only difference being the placement of the fluorine atom in the ring. Perhaps the position of the fluorine atom in the former probably hinders effective binding with the pocket residue forcing the molecule to adopt a conformation that allows only a single π-cation interaction with arginine 166 (**entry f, Figure 4**). It is known from the x-ray crystal structure that the pocket region of 2OZ5 is present in a P loop region flanked by alpha helix chains α7, α8 and α3A displayed in **Figure 6 (A)**. This comparable lid of α7– α8 hairpin in located on one side of the entrance to the to the active site and helix α3A on the hydrophobic surface of pocket region and protects the catalytic Cys160 amino acid present within the P-loop PtpB resists oxidative inactivation better than the PtpA enzyme that does not possess this comparable lid.[18] As observed in **Figure 5a**, the more potent compound **5c** is placed nearer to the important catalytic residue Cys 160 in the binding pocket whereas the aromatic ring of **5b** lies in a different plane (**Figure 5b**).

Compounds **4a**, **5c**, **5d**, rifampicin and ethambutol interacted with Arg166 and Ser57 residues in the pocket region of phosphotyrosine phosphatase B protein. After post filtering process, the top docked protein conformation for compound **5c** was chosen. **Figure 6(B)** highlights the top docked pose of compound **5c** aligned to the native ligand pose. Structure alignment of conformations was performed using Pymol v1.7.6. Similarity in alignment between the compounds suggests that the top docked conformation of **5c** is closer to the native bioactive conformation. **Figure 6(C)** shows the orientations of the compounds **5c** and native ligand in the binding pocket of the receptor.

Chemoinformatics Analysis

A druggability check was performed for all the 15 synthesized compounds (**Table 4**). Lipinski rule of 5 predictions were performed using the Screening Assistant 2 tool.[19] Most compounds displayed no violation of the standard Rule of 5 indicating that they possess good drug like properties.[20] The notion that these compounds could be further developed as anti-tubercular compounds was further affirmed by ADME properties prediction using PreADMET software.[21] The compounds clearly lie in the acceptable range of BBB model suggesting that the compounds can penetrate the Blood Brain Barrier. It is well established fact that for a compound to be accepted in an oral dosage form, Caco2 cell permeability values should be above 25nms[22] and the Human Intestinal Absorption(HIA) quantities should lie in the 50-100% range.[23] The selected compound **5c**, prioritized in this study fulfilled the above criteria. TPSA (Topological polar surface area) results indicated satisfactory values for all the 15 compounds. LAZAR (Lazy structure activity relationships) software detects mutagenic and/or carcinogenic properties based on the similarities in functional group with mutagenic and/or carcinogenic compounds present in the Lazar database.[24] Based on this software, all the compounds were predicted to be non-carcinogenic and non-mutagenic wherein the confidence value greater than 0.025 suggested the model to give highly reliable predictions. Thus most synthesized compounds predicted favorable ADME predictions. To further corroborate our studies, an in-house developed integrated suite of programs–ChemScreener was employed. The program rapidly annotates huge chemical libraries with more than thousand pharmacophoric (P), toxicophoric (T) and chemophoric (C) attributes to prioritize compounds in a virtual screening run.[25] The significance of the presence of pharmacophore and toxicophore features in a molecule is commonly known in the medicinal chemistry literature, the term 'chemophore' refers to groups that are too reactive or inert. A judicious selection of these features in a molecule will impact its further development as a drug. The ChemScreener results for the compounds **5b**, **5c** and **5d** yielded a PTC score of 56, 33 and 25 indicating that they possess an optimum combination of maximum pharmacophoric features and low toxicophoric and chemophoric features. Based on the comprehensive studies performed it is reasonable to state that the active compounds can be further developed as lead molecules against tuberculosis.

QSAR Modeling

We applied the QSAR approach to model the bioactivity of the chalcones in our quest to gather some clues regarding the molecular characteristics essential for biological activity. Initially, a simple 2D regression model was built using PLS approach for the series of chalcones using physico-chemical 2D structural descriptors implemented in MOE package[26] which yielded a coefficient of determination 0.9449 and a root mean square error (RMSE) value of 1.70 (**Figure S1**). Next, we computed the 3D QM/QC based descriptors using PM3 and AM1 Hamiltonian for studying the electronic properties with an objective of mapping them with the variation in activity. The molecules were geometry optimized and subjected to energy minimization by employing the MMFF94x force field. The resultant 3D QSAR model yielded a R^2 value of 0.87507, RMSE 2.72 and a cross validated $R^2(Q^2)$ value of 0.687. The decrease in r squared value in the latter case can be attributed to the presence of few outliers such as compound **5b** which showed better fit with 2D rather than 3D descriptors (**Figure S2**).

For a comprehensive list of all the descriptors and their computed values, please refer to the Supplementary Table S1. In the 3D model it was observed that the main properties correlating with the biological activity were the molecular orbital energies such as E(LUMO), E(HOMO). Frontier orbitals of valence electrons of compounds are known to play a major role in governing affinity towards biomolecules, specifically low values of LUMO indicate good electron acceptor tendency of the molecule and facilitate better interactions with the residue atoms in the active site of the receptor which eventually determine the biological activity. The molecules with lower ELUMO values were found to possess better biological activities. (See entries 1, 9-11, **Table S1**). All these molecules possess a halogen atom (X= F, Cl) on the benzene ring moiety. It is to be noted here that the docking studies also revealed the halogen substituted benzene ring to be involved in an arene cation type of interaction with the receptor residue atoms. The presence of a methoxy group in the benzene system on the other hand increased the E(LUMO) energies without affecting the E(HOMO) energies (entries 4,5,6) however when the piperidine group was present on the spiro skeleton, the methoxy group effect on the energies was not so prominent. It thus appears that the concurrent presence of halogen on the benzene ring moiety and piperidine on the spiro conjugated framework of the molecular system is essential for eliciting the bioactivity. A Genetic Programming based Symbolic Regression (GP-SR)[27,28] modelling was performed to verify the correlation of electronic energy descriptors with bioactivity. The GP model produced a Correlation Coefficient (CC) value of 0.9757, 0.0684(RMSE) and 1.7353 (MAPE). The GP expression obtained is shown in the equation (1), parity plot of experimental versus GP predicted values is given in the Supplementary Information (**Figure S3**).

$$X = \frac{15.14+1.634*A}{0.836+B} - 473.985 - (11.894*E) - (44.639*C) - (128.475*D) - (459.094*B) - (13.89*D*E) - (53.352*C*B)$$

Equation 1 (Where A= PM3_HOMO, B= PM3_LUMO, C=AM1_HOMO, D= AM1_LUMO,E=MNDO_HOMO and X= Bioactivity (MIC, µg/mL)

Thus the electronic energy descriptors based QSAR model developed can be employed in near future for virtual screening of not yet synthesized chalcone skeleton based molecules. To provide an in-depth analysis of molecular orbitals and derive more accurate energies, ab initio method was employed using DFT level of theory,

Journal Name

ARTICLE

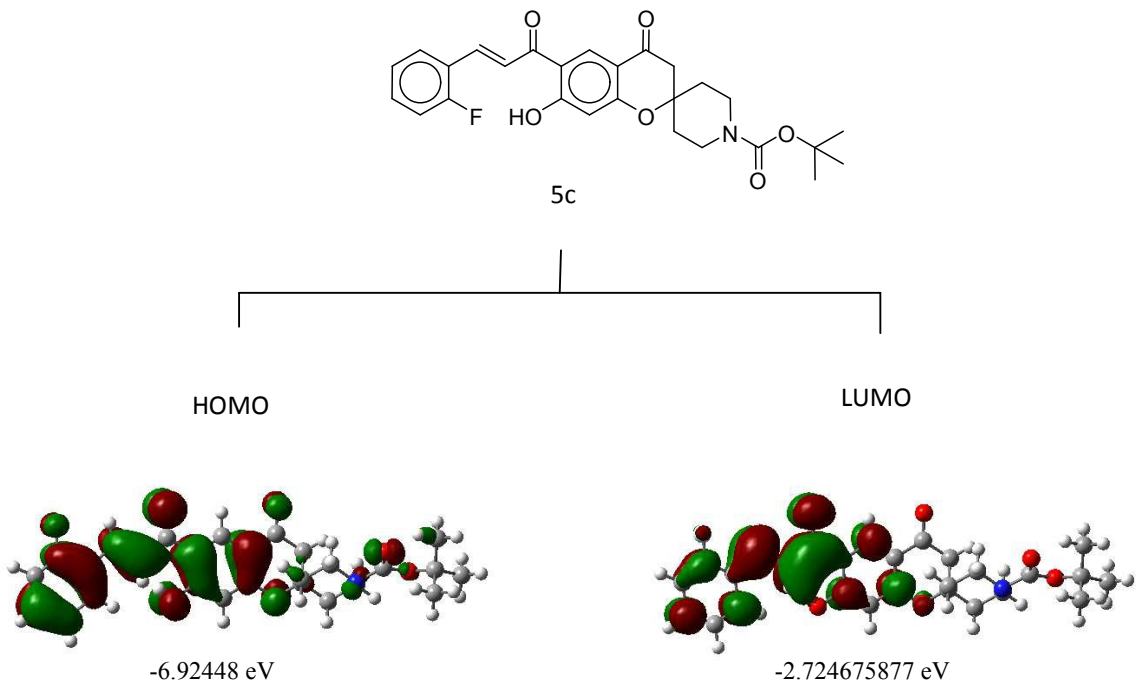

Figure 7: Iso density surface maps of frontier orbitals of molecule **5c** with best inhibitory activity as determined in the *in vitro Mtb* assay.

B3LYP functional and 6-31G basis set. The HOMO LUMO energies in Gaussian 09[29] were -6.92448 eV and -2.724675877 eV respectively. The iso density surface plots of HOMO and LUMO for the compound **5c** possessing the best inhibitory activity are depicted in the **Figure 7**. The HOMOs lie over the tricyclic spiro-chromone ring system while the LUMOs are located over the fluoro benzene ring moiety in the molecule.

Conclusion

In summary, a series of spirochromone annulated chalcone conjugates were synthesized for the first time using an efficient synthetic procedure beginning from resorcinol. All these new compounds were characterized by ^{1}H NMR, ^{13}C NMR and mass spectral analysis. The *in vitro* antimycobacterial evaluation of all the synthesized compounds showed that five compounds possess moderate to good antimycobacterial activity. Noticeably, compound **5c** is most potent compound *in vitro* with a MIC value of 3.13 µg/mL, against MTB. Molecular docking studies were utilized to explore the putative targets among the known chalcone specific protein receptors. In theory the compounds showed greater affinity towards the mycobacterium phosphatase Ptp B enzyme, these studies will provide guidelines for future experimental efforts. Chemoinformatics analysis using a host of known and internally developed tools indicated that the compounds prioritized in this study possess good ADME profile, low toxicity and high pharmacophoric attributes essential for further development as anti-tubercular agents. Further, QSAR modeling established the correlation between frontier molecular orbital energies and biological activities of the compounds. The GP based expression can be used for screening new molecules for their therapeutic action.

Experimental Section

General Methods

Solvents were purified and dried by standard procedures prior to use. ^{1}H NMR and ^{13}C NMR spectra were recorded on a Bruker AC-200 NMR spectrometer. Spectra were obtained in CDCl3. Monitoring of reactions was carried out using TLC plates Merck Silica gel 60 F254 and visualization with UV light (254 and 365 nm), I2 and anisaldehyde in ethanol as development reagents. HRMS (ESI) were recorded on a ORBITRAP mass analyser (Thermo Scientific, QExactive). Mass spectra were recorded at an ionization energy 70 eV on API Q Star Pulsar spectrometer using electrospray ionization. Ten fold serial dilutions of each test compound/drug

were incorporated into Middlebrook 7H11 agar medium with OADC Growth Supplement. Inoculum of M. tuberculosis H37Rv were prepared from fresh Middlebrook 7H11 agar slants with OADC Growth Supplement adjusted to 1mg/mL (wet weight) in Tween 80 (0.05%) saline diluted to 100-2 to give a concentration of approximately 1007 cfu/mL. A 5 µL amount of bacterial suspension was spotted into 7H11 agar tubes containing 10-fold serial dilutions of drugs per mL. The tubes were incubated at 37 °C, and final readings were recorded after 28 days. The minimum inhibitory concentration (MIC) is defined as the minimum concentration of compound required to give complete inhibition of bacterial growth.

1,1'-(4,6-dihydroxy-1,3-phenylene)bis(ethan-1-one) (2)

To a mixture of resorcinol (5 g, 45.5 mmol) and acetic anhydride (9.3 g, 91 mmol) was added zinc chloride (10 g, 73.4 mmol) and the resulting mixture was heated at 140 °C for 30 minutes. The hot mixture was allowed to attain ambient temperature followed by addition of 50% dilute HCl (140 mL) and the solution was allowed to stand for 1 h. The orange crude product was obtained by filtration with suction, washed with distilled water till the colour of the filtrate is nearly colourless. The crude product was crystallized using ethanol to yield 4,6-diacetylresorcinol **2** (6.6 g, 75%); m.p. 178-79 ^{o}C; ^{1}H NMR (200 MHz, $CDCl_3$): δ_H = 2.64 (s, 6H), 6.42 (s, 1H), 8.21 (s, 1H), 12.93 (s, 2H); ^{13}C NMR (50 MHz, $CDCl_3$): δ 202.4 (CO, 2 carbons), 168.8 (C, 2 carbons), 136.2 (CH, 2 carbons), 113.5 (C), 104.9 (CH), 26.0 (CH_3, 2 carbons).

6-acetyl-7-hydroxyspiro[chromane-2,1'-cyclohexan]-4-one (3a)

To a solution of **2** (5 g, 24.7 mmol) in ethanol (20 mL) was added cyclohexanone (6 mL, 49 mmol) followed by addition of pyrollidine (5.7 mL, 49 mmol) and the resulting mixture was refluxed using Dean-Stark apparatus for 12 h. After completion of the reaction, solvent was removed under reduced pressure and the residue was dissolved in ethyl acetate. The organic layer was washed with 1N HCl followed by dilute $NaHCO_3$, brine and concentrated. The crude product was purified using column chromatography (silica gel, pet ether/ ethyl acetate, 95:5) to yield **3a** (4.2 g, 62%) as a colourless solid. ^{1}H NMR (200 MHz, $CDCl_3$): δ_H = 1.44-1.75 (m, 8H), 1.94-2.03 (m, 2H), 2.63 (s, 3H), 2.70 (s, 2H), 6.48 (s, 1H), 8.36 (s, 1H), 12.82 (s, 1H); ^{13}C NMR (50 MHz, $CDCl_3$): δ 203.3 (CO), 190.5 (CO), 168.6 (C), 165.1 (C), 131.8 (CH), 115.0 (C), 113.9 (C), 105.1 (CH), 81.3 (C), 47.7 (CH_2), 34.9 (CH_2, 2 carbons), 26.4 (CH_3), 24.9 (CH_2), 21.3 (CH_2, 2 carbons); MS: m/z 297 $[M+Na]^+$.

tert-butyl 6-acetyl-7-hydroxy-4-oxospiro[chromane-2,4'-piperidine]-1'-carboxylate (3b)

The same procedure as in the preparation of **3a** was used with the *N*-Boc piperidone (5.9 g, 21.5 mmol) affording spirocompound **3b** as a colorless solid (5.2 g, 65 %); m.p. 181-82 ^{o}C. ^{1}H NMR (200 MHz, $CDCl_3$): δ_H = 1.46 (s, 9H), 1.56-1.71 (m, 2H), 1.97-2.04 (m, 2H), 2.64 (s, 3H), 2.72 (s, 2H), 3.16-3.27 (m, 2H), 3.88-3.92 (m, 2H), 6.48 (s, 1H), 8.38 (s, 1H), 12.85 (s, 1H); ^{13}C NMR (50 MHz, $CDCl_3$): δ 203.6 (CO), 189.4 (CO), 168.8 (C), 164.4 (C), 154.5 (C), 131.9 (CH), 115.3 (C), 113.7 (C), 105.2 (CH), 79.8 (C), 79.1 (C), 47.6 (CH_2), 34.2 (CH_2), 28.3 (CH_3, 3 carbons), 26.4 (CH_3).

Synthesis of spirochromone annulated chalcone conjugates (4-5): General procedure:

To a well-stirred mixture of (**3a** or **3b**) (0.7 mmol) and substituted aldehydes (0.77 mmol) in methanol (3 mL) at room temperature was slowly added 50% KOH solution (5 mL) dropwise. The resulting reaction mixture was stirred for 12 h at 60 ^{o}C. After completion of the reaction (by TLC), solvent was removed under reduced pressure and the residue was dissolved in ethyl acetate. The organic layer was washed with 5% HCl followed by brine, dried and concentrated. The residue was purified by column chromatography (silica gel, pet ether/ ethyl acetate, 75:25) to yield pure product **4-5**. Spectroscopic data of compounds **4-5** are given below.

(E)-6-(3-(4-fluorophenyl)acryloyl)-7-hydroxyspiro[chromane-2,1'-cyclohexan]-4-one (4a)

Yellow solid; m.p. 156-57 ^{o}C, ^{1}H NMR (200 MHz, $CDCl_3$): δ_H = 1.46-1.77 (m, 8H), 1.97-2.05 (m, 2H), 2.73 (s, 2H), 6.50 (s, 1H), 6.95-7.19 (m, 2H), 7.51 (dd, *J* = 15.4, 9.3 Hz, 1H), 7.65-7.74 (m, 2H), 7.86 (dd, 15.4, 3.1Hz, 1H), 13.5 (s, 1H); ^{13}C NMR (50 MHz, $CDCl_3$): δ_C 192.3 (CO), 190.6 (CO), 169.9 (C), 165.2 (C), 161.8 (C), 144.4 (CH), 130.9 (CH, 2 carbons), 130.7 (CH), 130.6 (C), 119.2 (CH), 116.4 (CH, 2 carbons), 115.2 (C), 113.9 (C), 105.4 (CH), 81.4 (C), 47.8 (CH_2), 35.0 (CH_2, 2 carbons), 24.9 (CH_2), 21.3 (CH_2, 2 carbons); HRMS(ESI): m/z Calcd for $C_{23}H_{21}FO_4$ $[M+H]^+$ 381.1497, found 381.1495.

(E)-6-(3-(2-fluorophenyl)acryloyl)-7-hydroxyspiro[chromane-2,1'-cyclohexan]-4-one (4b)

Yellow solid; m.p. 188-89 ^{o}C; ^{1}H NMR (200 MHz, $CDCl_3$): δ_H = 1.46-1.77 (m, 8H), 1.97-2.03 (m, 2H), 2.73 (s, 2H), 6.50 (s, 1H), 6.95-7.24 (m, 2H), 7.38-7.49 (m, 1H), 7.69-7.82 (m, 2H), 8.03 (d, *J*=15.4 Hz, 1H), 8.55 (s, 1H), 13.49 (s, 1H); ^{13}C NMR (50 MHz, $CDCl_3$): δ_C = 192.6 (CO), 190.6 (CO), 170.0 (C), 165.3 (C), 159.3 (C), 138.2 (CH), 132.4 (CH), 130.8 (CH), 129.5(CH), 124.6 (CH), 122.0 (CH), 121.9 (C), 116.1 (CH), 115.3 (C), 114.0 (C), 105.4 (CH), 81.5 (C), 47.8 (CH_2), 35.1 (CH_2, 2 carbons), 25.0 (CH_2), 21.4 (CH_2, 2 carbons); HRMS(ESI): m/z Calcd for $C_{23}H_{21}FO_4$ $[M+H]^+$ 381.1497, found 381.1496.

(E)-6-(3-(2-chlorophenyl)acryloyl)-7-hydroxyspiro[chromane-2,1'-cyclohexan]-4-one (4c)

Yellow solid; m.p. 162-63 ^{o}C; ^{1}H NMR (200 MHz, $CDCl_3$): δ_H = 1.52-1.70 (m, 8H), 1.97-2.03 (m, 2H), 2.73 (s, 2H), 6.52 (s, 1H), 7.34-7.39 (m, 2H), 7.43-7.48 (m, 1H), 7.62 (d, *J* = 15.5 Hz, 1H), 7.82-7.86 (m, 1H), 8.30 (d, *J* = 15.5 Hz, 1H), 8.55 (s, 1H), 13.45 (s, 1H); ^{13}C NMR (50 MHz, $CDCl_3$): δ_C 192.2 (CO), 190.6 (CO), 170.0 (C), 165.3 (C), 141.4 (CH), 135.8 (C), 132.7 (C), 131.6 (CH), 130.7 (CH), 130.3 (CH), 128.0 (CH), 127.1 (CH), 122.0 (CH), 115.2 (C), 113.9 (C), 105.4 (CH), 81.4 (C), 47.8 (CH_2), 35.0 (CH_2, 2 carbons), 24.9 (CH_2), 21.3 (CH_2, 2 carbons); HRMS(ESI): m/z Calcd for $C_{23}H_{21}ClO_4$ $[M+H]^+$ 397.1201, found 397.1203.

(E)-7-hydroxy-6-(3-(4-methoxyphenyl)acryloyl)spiro[chromane-2,1'-cyclohexan]-4-one (4d)

Yellow solid; m.p. 164-65 ^{o}C; ^{1}H NMR (200 MHz, $CDCl_3$): δ_H = 1.47-1.67 (m, 8H), 1.96-2.03 (m, 2H), 2.72 (s, 2H), 3.87 (s, 3H), 6.50 (s, 1H), 6.94 (dd, *J* = 8.8, 2.8 Hz, 2H), 7.50 (d, *J* = 15.4 Hz, 1H), 7.63 (d, *J* = 7.8 Hz, 2H), 7.87 (dd, *J* = 15.2, 8.0 Hz, 1H), 8.55 (s, 1H), 13.73 (s,

1H); ^{13}C NMR (50 MHz, $CDCl_3$): δ_C 192.5 (CO), 190.7 (CO), 170.0 (C), 165.0 (C), 162.1 (C), 145.7 (CH), 130.8 (CH, 2 carbons), 130.7 (CH), 127.1 (C), 116.8 (CH), 115.3 (C), 114.5 (CH, 2 carbons), 113.8 (C), 105.3 (CH), 81.3 (C), 55.4 (CH_3), 47.8 (CH_2), 35.0 (CH_2, 2 carbons), 24.9 (CH_2), 21.3 (CH_2, 2 carbons); HRMS(ESI): m/z Calcd for $C_{23}H_{24}O_5$ $[M+H]^+$ 393.1697, found 393.1697.

(E)-6-(3-(2,4-dimethoxyphenyl)acryloyl)-7-hydroxyspiro[chromane-2,1'-cyclohexan]-4-one (4e)

Yellow solid; m.p. 215-16 °C; ^{1}H NMR (200 MHz, $CDCl_3$): δ_H = 1.51-1.77 (m, 8H), 1.97-2.03 (m, 2H), 2.71 (s, 2H), 3.88 (s, 3H), 3.93 (s, 3H), 6.48-6.49 (m, 2H), 6.54 (dd, *J* = 8.5, 2.4 Hz, 1H), 7.63 (d, *J* = 1.6 Hz, 1H), 7.67 (d, *J* = 8.6 Hz, 1H), 8.17 (d, *J* = 15.6 Hz, 1H), 8.56 (s, 1H), 13.88 (s, 1H); ^{13}C NMR (50 MHz, $CDCl_3$): δ_C 193.1 (CO), 190.7 (CO), 170.1 (C), 164.9 (C), 163.6 (C), 160.7 (C), 141.4 (CH), 131.3 (CH), 130.5 (CH), 117.3 (CH), 116.7 (C), 115.6 (C), 113.7 (C), 105.6 (CH), 105.2 (CH), 98.4 (CH), 81.2 (C), 55.6 (CH_3), 55.5 (CH_3), 47.9 (CH_2), 35.1 (CH_2, 2 carbons), 25.0 (CH_2), 21.4 (CH_2, 2 carbons); HRMS(ESI): m/z Calcd for $C_{25}H_{26}O_6$ $[M+H]^+$ 423.1802, found 423.1801.

(E)-7-hydroxy-6-(3-(3-methoxyphenyl)acryloyl)spiro[chromane-2,1'-cyclohexan]-4-one (4f)

Yellow solid; m.p. 162-63 °C; ^{1}H NMR (200 MHz, $CDCl_3$): δ_H = 1.48-1.70 (m, 8H), 1.97-2.04 (m, 2H), 2.73 (s, 2H), 3.90 (s, 3H), 6.52 (s, 1H), 6.98-7.04 (m, 1H), 7.19-7.20 (m, 1H), 7.28-7.42 (m, 2H), 7.61 (d, *J* = 15.4 Hz, 1H), 7.87 (d, *J* = 15.4 Hz, 1H), 8.57 (s, 1H), 13.50 (s, 1H); ^{13}C NMR (50 MHz, $CDCl_3$): δ_C 192.6 (CO), 190.6 (CO), 170.0 (C), 165.2 (C), 160.0 (C), 145.8 (CH), 130.7 (CH), 130.0 (CH), 121.5 (CH), 121.4 (C), 119.8 (CH), 117.1 (C), 117.0 (CH), 113.9 (C), 113.6 (CH), 105.4 (CH), 81.4 (C), 55.4 (CH_3), 47.8 (CH_2), 35.0 (CH_2, 2 carbons), 25.0 (CH_2), 21.3 (CH_2, 2 carbons); HRMS(ESI): m/z Calcd for $C_{25}H_{24}O_5$ $[M+H]^+$ 393.1697, found 393.1703.

(E)-6-(3-(benzo[d][1,3]dioxol-5-yl)acryloyl)-7-hydroxyspiro[chromane-2,1'-cyclohexan]-4-one (4g)

Yellow solid; m.p. 162-63 °C; ^{1}H NMR (200 MHz, $CDCl_3$): δ_H = 1.52-1.77 (m, 8H), 1.97-2.03 (m, 2H), 2.73 (s, 2H), 6.06 (m, 2H), 6.51 (s, 1H), 6.85 (d, *J* = 7.9 Hz, 1H), 7.17 (dd, *J* = 8.2, 1.2 Hz, 1H), 7.23-7.24 (m, 1H), 7.46 (d, *J* = 15.5 Hz, 1H), 7.82 (d, *J* = 15.5 Hz, 1H), 8.54 (s, 1H), 13.66 (s, 1H); ^{13}C NMR (50 MHz, $CDCl_3$): δ_C 192.4 (CO), 190.6 (CO), 170.0 (C), 165.1 (C), 150.4 (C), 148.5 (C), 145.6 (CH), 130.5 (CH), 128.8 (C), 125.8 (CH), 117.4 (CH), 115.3 (C), 113.8 (C), 108.7 (CH), 107.0 (CH), 105.3 (CH), 101.7 (CH_2), 81.3 (C), 47.8 (CH_2), 35.0 (CH_2, 2 carbons), 24.9 (CH_2), 21.3 (CH_2, 2 carbons); HRMS(ESI): m/z Calcd for $C_{24}H_{22}O_6$ $[M+H]^+$ 407.1489, found 407.1489.

tert-butyl 6-cinnamoyl-7-hydroxy-4-oxospiro[chromane-2,4'-piperidine]-1'-carboxylate (5a)

Yellow solid; m.p. 165-66 °C; ^{1}H NMR (200 MHz, $CDCl_3$): δ_H = 1.47 (s, 9H), 1.61-1.69 (m, 2H), 1.99-2.04 (m, 2H), 2.75 (s, 2H), 3.22-3.24 (m, 2H), 3.87-3.96 (m, 2H), 6.54 (s, 1H), 7.46-7.47 (m, 3H), 7.66-7.72 (m, 3H), 7.94 (d, *J* = 15.5 Hz, 1H), 8.59 (s, 1H), 13.58 (s, 1H); ^{13}C NMR (50 MHz, $CDCl_3$): δ_C 192.6 (CO), 189.6 (CO), 170.2 (C), 164.4 (C),154.6 (CO), 146.1 (CH), 134.3 (C), 131.2 (CH), 130.8 (CH), 129.0 (CH, 2 carbons), 128.9 (CH, 2 carbons), 119.3 (CH), 115.7 (C), 113.7 (C), 105.5 (CH), 79.9 (C), 79.2 (C), 47.7 (CH_2, 2 carbons), 47.6 (CH_2), 34.2 (CH_2, 2 carbons), 28.3 (CH_3, 3 carbons); HRMS(ESI): m/z Calcd for $C_{27}H_{29}NO_6$ $[M+Na]^+$ 486.1887, found 486.1897.

tert-butyl (E)-6-(3-(4-fluorophenyl)acryloyl)-7-hydroxy-4-oxospiro[chromane-2,4'-piperidine]-1'-carboxylate (5b)

Yellow solid; m.p. 177-78 °C; ^{1}H NMR (400 MHz, $CDCl_3$): δ_H = 1.47 (s, 9H), 1.63-1.69 (m, 2H), 2.02 (bd, *J* = 13.7 Hz, 2H), 2.74 (s, 2H), 3.21-3.24 (m, 2H), 4.09-4.14 (m, 2H), 6.53 (s, 1H), 6.96 (d, *J* = 8.1 Hz, 2H), 7.54 (d, *J* = 15.2 Hz, 1H), 7.66 (d, *J* = 8.5 Hz, 2H), 7.93 (d, *J* = 15.1 Hz, 1H), 8.57 (s, 1H), 13.77 (s, 1H); ^{13}C NMR (100 MHz, $CDCl_3$): δ_C 192.6 (CO), 189.7 (CO), 170.3 (C), 164.3 (C), 161.7 (C), 154.6 (CO), 146.2 (CH), 130.9 (CH, 2 carbons), 130.6 (C), 126.9 (CH), 116.6 (CH), 115.8 (C), 115.0 (C), 113.6 (CH, 2 carbons), 105.4 (CH), 79.9 (C), 79.1 (C), 47.7 (CH_2, 3 carbons), 34.3 (CH_2, 2 carbons), 28.4 (CH_3, 3 carbons); HRMS(ESI): m/z Calcd for $C_{27}H_{28}FNO_6$ $[M+Na]^+$ 504.1793, found 504.1798.

tert-butyl (E)-6-(3-(2-fluorophenyl)acryloyl)-7-hydroxy-4-oxospiro[chromane-2,4'-piperidine]-1'-carboxylate (5c)

Yellow solid; m.p. 174-75 °C; ^{1}H NMR (200 MHz, $CDCl_3$): δ_H = 1.47 (s, 9H), 1.63-1.69 (m, 2H), 2.01-2.05 (m, 2H), 2.75 (s, 2H), 3.21-3.24 (m, 2H), 3.89-3.90 (m, 2H), 6.54 (s, 1H), 7.14-7.25 (m, 2H), 7.42-7.47 (m, 1H), 7.71-7.78 (m, 2H), 8.06 (d, *J* = 15.4 Hz, 1H), 8.57 (s, 1H), 13.50 (s, 1H); ^{13}C NMR (50 MHz, $CDCl_3$): δ_C 192.6 (CO), 189.5 (CO), 170.1 (C), 164.5 (C), 160.5 (C), 154.6 (CO), 138.5 (CH), 130.9 (C), 129.6 (CH), 124.6 (CH), 122.4 (C), 121.8 (CH), 116.4 (CH), 116.2 (CH) 115.6 (C), 113.7 (C), 105.5 (CH), 79.9 (C), 79.2 (C), 47.7 (CH_2, 3 carbons), 34.3 (CH_2, 2 carbons), 28.3 (CH_3, 3 carbons); HRMS(ESI): m/z Calcd for $C_{27}H_{28}FNO_6$ $[M+Na]^+$ 504.1793, found 504.1792.

tert-butyl (E)-6-(3-(2-chlorophenyl)acryloyl)-7-hydroxy-4-oxospiro[chromane-2,4'-piperidine]-1'-carboxylate (5d)

Yellow solid; m.p. 183-84 °C; ^{1}H NMR (200 MHz, $CDCl_3$): δ_H = 1.47 (s, 9H), 1.58-1.73 (m, 2H), 2.00-2.05 (m, 2H), 2.75 (s, 2H), 3.17-3.29 (m, 2H), 3.88-3.93 (m, 2H), 6.55 (s, 1H), 7.36-7.50 (m, 3H), 7.61 (d, *J* = 15.5 Hz, 1H), 7.82-7.87 (m, 1H), 8.33 (d, *J* = 15.5 Hz, 1H), 8.57 (s, 1H), 13.49 (s, 1H); ^{13}C NMR (50 MHz, $CDCl_3$): δ_C 192.3 (CO), 189.5 (CO), 170.1 (C), 164.5 (C), 159.3 (C), 154.6 (CO), 141.7 (CH), 135.8 (C), 132.6 (C), 131.8 (CH), 130.9 (CH), 130.4 (CH), 128.0 (CH), 127.2 (CH), 121.9 (CH), 113.7 (C), 105.5 (CH), 79.9 (C), 79.2 (C), 47.7 (CH_2, 3 carbons), 34.3 (CH_2, 2 carbons), 28.3 (CH_3, 3 carbons); HRMS(ESI): m/z Calcd for $C_{27}H_{28}ClNO_6$ $[M+Na]^+$ 520.1497, found 520.1500.

tert-butyl (E)-7-hydroxy-6-(3-(3-methoxyphenyl)acryloyl)-4-oxospiro[chromane-2,4'-piperidine]-1'-carboxylate (5e)

Yellow solid; m.p. 162-63 °C; ^{1}H NMR (200 MHz, $CDCl_3$): δ_H = 1.47 (s, 9H), 1.61-1.67 (m, 2H), 2.00-2.07 (m, 2H), 2.73 (s, 2H), 3.16-3.29 (m, 2H), 3.84-3.89 (m, 5H), 6.52 (s, 1H), 6.96-7.02 (m, 1H), 7.17-7.20 (m, 1H), 7.31-7.41 (m, 2H), 7.59 (d, *J* = 15.2 Hz, 1H), 7.87 (d, *J* = 15.2 Hz, 1H), 8.56 (s, 1H), 13.56 (s, 1H); ^{13}C NMR (50 MHz, $CDCl_3$): δ_C 192.6 (CO), 189.5 (CO), 170.2 (C), 164.5 (C), 160.3 (C), 154.6 (CO), 146.2 (CH), 135.6 (CH), 130.8 (CH), 130.0 (CH), 121.5 (CH), 119.6 (C), 117.1

(CH), 115.7 (C), 113.7 (CH), 113.7 (C), 105.5 (CH), 79.9 (C), 79.2 (C), 55.4 (CH_3), 47.7 (CH_2, 3 carbons), 34.3 (CH_2, 2 carbons), 28.3 (CH_3, 3 carbons); HRMS(ESI): m/z Calcd for $C_{28}H_{31}NO_7$ $[M+Na]^+$ 516.1993, found 516.2006.

tert-butyl (E)-7-hydroxy-6-(3-(4-methoxyphenyl)acryloyl)-4-oxo spiro[chromane-2,4'-piperidine]-1'-carboxylate (5f)

Yellow solid; m.p. 176-77 °C; ^{1}H NMR (200 MHz, $CDCl_3$): δ_H = 1.47 (s, 9H), 1.60-1.73 (m, 2H), 2.00-2.06 (m, 2H), 2.74 (s, 2H), 3.18-3.29 (m, 2H), 3.89-3.90 (m, 5H), 6.53 (s, 1H), 6.95 (d, *J* = 8.7 Hz, 2H), 7.50 (d, *J* = 15.7 Hz, 1H), 7.65 (d, *J* = 8.7 Hz, 2H), 7.89 (d, *J* = 15.7 Hz, 1H), 8.58 (s, 1H), 13.76 (s, 1H); ^{13}C NMR (50 MHz, $CDCl_3$): δ_C 192.5 (CO), 189.7 (CO), 170.2 (C), 164.2 (C), 162.2 (C), 154.6 (CO), 146.0 (CH), 130.8 (CH, 2 carbons), 130.6 (CH), 127.0 (C), 116.7 (CH), 115.7 (C), 114.4 (CH, 2 carbons), 113.5 (C), 105.3 (CH), 79.9 (C), 79.0 (C), 55.4 (CH_3), 47.6 (CH_2, 3 carbons), 34.3 (CH_2, 2 carbons), 28.4 (CH_3, 3 carbons); HRMS(ESI): m/z Calcd for $C_{28}H_{31}NO_7$ $[M+H]^+$ 494.2173, found 494.2175.

tert-butyl (E)-6-(3-(2,4-dimethoxyphenyl)acryloyl)-7-hydroxy-4-oxospiro[chromane-2,4'-piperidine]-1'-carboxylate (5g)

Yellow solid; m.p. 160-61 °C; ^{1}H NMR (200 MHz, $CDCl_3$): δ_H = 1.47 (s, 9H), 1.66-1.72 (m, 2H), 1.99-2.05 (m, 2H), 2.73 (s, 2H), 3.16-3.31 (m, 2H), 3.88-3.89 (m, 5H), 3.93 (s, 3H), 6.48-6.49 (m, 1H), 6.51 (s, 1H), 6.54-6.60 (m, 1H), 7.62-7.63 (m, 1H), 7.67 (d, *J* = 8.1 Hz, 1H), 8.18 (d, *J* = 15.4 Hz, 1H), 8.57 (s, 1H), 13.93 (s, 1H); ^{13}C NMR (50 MHz, $CDCl_3$): δ_C 193.0 (CO), 189.7 (CO), 170.3 (C), 164.1 (C), 163.7 (C), 160.7 (C), 154.6 (CO), 141.7 (CH), 131.3 (CH), 130.6 (CH), 116.9 (CH), 116.5 (C), 115.9 (C), 113.5 (C), 105.5 (CH), 105.3 (CH), 98.3 (CH), 79.8 (C), 78.9 (C), 55.6 (CH_3), 55.5 (CH_3), 47.7 (CH_2, 3 carbons), 34.2 (CH_2, 2 carbons), 28.3 (CH_3, 3 carbons); HRMS(ESI): m/z Calcd for $C_{29}H_{33}NO_8$ $[M+Na]^+$ 546.2098, found 546.2126.

tert-butyl (E)-6-(3-(2,5-dimethoxyphenyl)acryloyl)-7-hydroxy-4-oxospiro[chromane-2,4'-piperidine]-1'-carboxylate (5h)

Yellow solid; m.p. 150-51 °C; ^{1}H NMR (200 MHz, $CDCl_3$): δ_H = 1.47 (s, 9H), 1.70-1.72 (m, 2H), 2.00-2.07 (m, 2H), 2.74 (s, 2H), 3.16-3.29 (m, 2H), 3.84-3.86 (m, 5H), 3.91 (s, 3H), 6.53 (s, 1H), 6.88-7.03 (m, 2H), 7.19 (d, *J* = 3.0 Hz, 1H), 7.70 (d, *J* = 15.4 Hz, 1H), 8.21 (d, *J* = 15.4 Hz, 1H), 8.59 (s, 1H), 13.72 (s, 1H); ^{13}C NMR (50 MHz, $CDCl_3$): δ_C 193.0 (CO), 189.5 (CO), 170.1 (C), 164.3 (C), 154.5 (CO), 153.6 (C), 153.4 (C), 141.4 (CH), 130.8 (CH), 123.7 (C), 120.0 (CH), 118.2 (CH), 115.8 (C), 113.7 (CH), 113.6 (C), 112.4 (CH), 105.3 (CH), 79.8 (C), 79.0 (C), 56.0 (CH_3), 55.9 (CH_3), 47.7 (CH_2), 47.6 (CH_2, 2 carbons), 34.2 (CH_2, 2 carbons), 28.3 (CH_3, 3 carbons); HRMS(ESI): m/z Calcd for $C_{29}H_{33}NO_8$ $[M+Na]^+$ 546.2098, found 546.2099.

Acknowledgments

Financial support from the CSIR Network projects (CSC0130, BSC0121 and CSC0108) is gratefully acknowledged. J. Robles acknowledges financial support from CONACYT (Research grant 168474). U.M.V.-B. (378051/252139). E. D.-C. acknowledges support from CONACYT graduate scholarship (368973/250842). L. C.-B. acknowledges support from CONACYT graduate scholarship (327057/265238). RV thanks DST, New Delhi for the award of a women scientist fellowship (LS-201/2011). All the authors thank the anonymous referee for providing suggestions to improve the manuscript.

Notes and references

1 (a) Global Tuberculosis Report 2014, World Health Organization, Geneva, 2014; (b) A. Koul, E. Arnoult, N. Lounis, J. Guillemont and K. Andries *Nature* **2011**, *469*, 483.

2 (a) D. J. Newman and G. M. Cragg, in Natural Products in Medicinal Chemistry, ed. S. Hanessian, Wiley-VCH Verlag GmbH & Co. KgaA, 1st edn., 2014, part.1, pp 1-41; (b) S. Basu, B. Ellinger, S. Rizzo, C. Deraeve, M. Schurmann, H. Preut, H. D. Arndt and H. Waldmann, *Proc. Nat. Acad. Sci.,* **2011**, *108*, 6805; (c) S. Wetzel, R. S. Bon, K. Kumar and H. Waldmann, *Angew. Chem. Int. Ed.,* **2011**, *50*, 10800; (d) M. Manger, M. Scheck, H. Prinz, J. P. V. Kries, T. Langer, K. Saxena, H. Schwalbe, A. Furstner, J. Rademann and H. Waldmann, *Chem Bio Chem.,* **2005**, *6*, 1749.

3 J. K. Lin and M. S. Weng, in The Science of Flavonoids, ed. E. Grotewold, Springer, New York, 2006, Ch. 8, pp 239-268.

4 (a) D. N. Dhar, The Chemistry of Chalcones and Related Compounds, John Wiley & Sons, New York, 1981.

5 L. D. Chiaradia, A. Mascarello, M. Purificacao, J. Vernal, M. N. S. Cordeiro, M. E. Zenteno, A. Villarino, R. J. Nunes, R. A. Yunes and H. Terenzi, *Bioorg. Med. Chem. Lett*., **2008**, *18*, 6227.

6 (a) Y. M. Lin, PCT, WO 01/21164A2, 2001; (b) Y. M. Lin, Y. Zhou, M. T. Flavin, L. M. Zhou, W. Nie and F. C. Chen, *Bioorg. Med. Chem.*, **2002**, *10*, 2795; (c) Z. Nowakowska, *Eur. J. Med. Chem.,* **2007**, *42*, 125; (d) R. H. Hans, E. M. Guantai, C. Lategan, P. J. Smith, B. Wan, S. G. Franzblau, J. Gut, R. J. Rosenthal and K. Chibale, *Bioorg. Med. Chem. Lett.,* **2010**, *20*, 942.

7 (a) L. D. Chiaradia, P. G. A. Martins, M. N. S. Cordeiro, R. V. C. Guido, G. Ecco, A. D. Andricopulo, R. A. Yunes, J. Vernal, R. J. Nunes and H. Terenzi, *J. Med. Chem*., **2012**, *55*, 390; (b) A. Mascarello, M. Mori, L. D. Chiaradia-Delatorre, A. C. O. Menegatti, M. F. Delle, F. Ferrari, R. A. Yunes, R. J. Nunes, H. Terenzi, B. Botta and M. Botta, *PLoS One*, **2013**, 8, e77081; (c) A. Mascarello, L. D. Chiaradia, J. Vernal, A. Villarino, R. V. C. Guido, P. Perizzolo, V. Poirier, D. Wong, P. G. A. Martins, R. J. Nunes, R. A. Yunes, A. D. Andricopulo, Y. Av-Gay and H. Terenzi, *Bioorg. Med. Chem*., **2010**, *18*, 3783.

8 B. W. Vanhoecke, F. Delporte, E. Van Braeckel, A. Heyerick, H. T. Depypere, M. Nuytinck, D. De Keukeleire, and M. E. Bracke, *In Vivo*. **2005**, *19*, 103.

9 (a) M. Muthukrishnan, U. M. V. Basavanag and V. G. Puranik, *Tetrahedron Lett*. **2009**, *50*, 2643; (b) M. Muthukrishnan and O. V. Singh, *Synth. Commun.* **2008**, *38*, 3875; (c) M. Muthukrishnan, P. S. Patil, S. V. More and R. A. Joshi, *Mendeleev Commun.* **2005**, 100; (d) O. V. Singh, M. Muthukrishnan and R. Gopan, *Synth. Commun.* **2005**, *35*, 2723; (e) O. V. Singh, M. Muthukrishnan and M. Sundaravadivelu, *Indian J. Chem.* **2005**, *44B*, 2575; (f) R. Vyas, M. Karthikeyan, G. Nainaru and M. Muthukrishnan *J Comb. H. Tr. Scrn*., **2015**, *18,* 624.

10 (a) M. Muthukrishnan, M. Mujahid, P. Yogeeswari and D. Sriram, *Tetrahedron Lett.* **2011**, *52*, 2387; (b) M. Mujahid, R. G. Gonnade, P. Yogeeswari and D. Sriram, M. Muthukrishnan, *Bioorg. Med. Chem. Lett.*, **2013**, *23*, 1416.

11 A. A. A. Emara and A. A. A. Abou-Hussen, *Spectrochim Acta A*. **2006**, *64*, 1010.

12 ChemAxon Marvin Suite 15 (Accessed on: 17th June 2015:https://www.chemaxon.com/download/marvin-suite/)

13 O. Trott, A. J. Olson, *Journal of Comput. Chem.* **2010**, *31*, 455.

14 Chemical Computing Group Inc., Molecular Operating Environment Software, Montreal, 2010.
15 F. Macaev, V. Boldescu, S. Pogrebnoi and G. Duca, *Medicinal Chemistry*, **2014**, *4*, 487.
16 C. Grundner, H. L. Ng and T. Alber, *Structure*, **2005**, *13*, 1625.
17 C. Grundner, D. Perrin, R. H. Van Huijsduijnen, D. Swinnen, J. Gonzalez, C. L. Gee and T. Alber, *Structure*, **2007**, *15*, 499.
18 K. A. Rawls, P. T. Lang, J. Takeuchi, S. Imamura, T. D. Baguley, C. Grundner, T. Alber and J. A. Ellman. *Bioorganic & Medicinal Chemistry Letters* **2009**, *19*, 6851.
19 V. Le Guilloux, A. Arrault, L. Colliandre, S. Bourg, P. Vayer and L. Morin-Allory, *J. cheminformatics*, **2012**, *4,* 20.
20 C. A. Lipinski, *Drug Discovery Today: Technologies*, **2004**, *1*, 337.
21 S.K. Lee, S. H. Park, I. H. Lee and No, K. T. PreAD-MET Ver. v2. 0, BMDRC: **2007**, Seoul. *Korea*.
22 M. Tripathi, S. I. Khan, A. Thakur, P. Ponnan and D. S. Rawat, *New J. Chem.*, **2015**, *39*, 3474.
23 S. Ren and E. J. Lien, Caco-2 cell permeability vs human gastro-intestinal absorption: QSPR analysis. In *Progress in Drug Research* (pp. 1-23), **2000**, Birkhäuser Basel.
24 A. Maunz, M. Gutlein, M. Rautenberg, D. Vorgrimmler, D. Gebele and C. Helma *Fron. Pharmacol.* **2013**, *4,* 38.
25 M. Karthikeyan, D. Pandit and R. Vyas, *J Comb. H. Tr. Scrn.*, **2015**, *18,* 544.
26 *Molecular Operating Environment (MOE)*, 2013.08; Chemical Computing Group Inc., 1010 Sherbooke St. West, Suite #910, Montreal, QC, Canada, H3A 2R7, **2015**.
27 R. Vyas, P. Goel, M Karthikeyan, S.S. Tambe and B.D. Kulkarni, *Lett. Drug Des. Discov.* **2014**, *11*, 1112.
28 R. Vyas, P. Goel and S. Tambe. Applications of genetic programming in chemistry and chemical engineering, in: A.H. Gandomi, A.H. Alavi, C. Ruan (Eds). Handbook of Genetic Programming applications, Springer, 2015, http://dx.doi.org/10.1007/978-3-319-20883-1-5, Chapter 5 (in press).
29 M. J. Frisch et al., Gaussian 09, Revision A.01, Gaussian Inc,

Graphical Abstract

Spirochromone-chalcone conjugates as antitubercular agents: synthesis, bio evaluation and molecular modeling studies

M. Mujahid, P. Yogeeswari, D. Sriram, U. M. V. Basavanag, Erik Díaz-Cervantes, Luis Córdoba-Bahena, Juvencio Robles, R. G. Gonnade, M. Karthikeyan, Renu Vyas and M. Muthukrishnan

We report new spiro chromone scaffold derived molecules possessing *invitro* anti-tubercular activities. QSAR based molecular modeling studies correlated the bioactivities with the frontier molecular orbital energies.